can eliminate the spatial effects that are of primary interest. For individual-based models (which operate at the level of the individual) and metapopulation models (which consider communities as the aggregate unit), the scale is generally fixed. However, for both lattice-based and continuous-space models (PDEs and IDEs), the question of scale is much more subtle. In such models, it is frequently assumed that each population interacts only with a limited number of other populations (usually within a prescribed distance), and this set of populations is referred to as the (interaction) *neighborhood*. In general, the use of a finite neighborhood is an approximation to the true dynamics, but may greatly increase the speed of any spatial simulation.

When dealing with a particular "real-world" problem, such as foot-and-mouth in the United Kingdom or SARS in North America, the spatial extent of our model is fixed by the problem. However, in more abstract or generic situations, the scale at which the spatial model operates is less constrained. Intuitively, we wish to model at a sufficiently large scale so that the full range of dynamics is observed and the scale of the model has limited impact on our results. However, models that are too "big" may be slow to compute, thereby limiting their usefulness. Finding the correct scale usually involves assessing whether the salient behavior of large-scale models is still captured by models of a smaller, more computationally manageable scale. Therefore, at least initially, large-scale simulations are required to determine the unconstrained dynamics. Although a number of dynamical systems techniques exist to find the optimal, most informative scale (Mead 1974; Keeling et al. 1997a; Pascual et al. 2001), the answer is often context dependant.

Assessing the fine scale at which individuals are aggregated and the larger scale at which simulations are performed should either be based on sound epidemiological knowledge or achieved by comparing simulated results across a range of scales.

7.2. METAPOPULATIONS

Metapopulations are one of the simplest spatial models, but are also one of the most applicable to modeling many human diseases. The metapopulation concept is to subdivide the entire population into distinct "subpopulations", each of which has independent dynamics, together with limited interaction between the subpopulations. This approach has been used to great effect within the ecological literature; a comprehensive guide to the broader applications of this approach is given by Hanski and Gilpin (1991, 1997) and Hanski and Goggiotti (2004). For disease-based metapopulation models, a suitable modified version of the SIR equation (Chapter 2) would be:

$$\begin{aligned} \frac{dX_i}{dt} &= \nu_i N_i - \lambda_i X_i - \mu_i X_i, \\ \frac{dY_i}{dt} &= \lambda_i X_i - \gamma_i Y_i - \mu_i Y_i, \end{aligned} \tag{7.3}$$

where the subscript i defines parameters and variables that are particular to subpopulation i. The force of infection, λ_i incorporates transmission from both the number of infecteds within subpopulation i and the coupling to other subpopulations. In this general formulation, the demographic and epidemiological parameters may vary between subpopulations,

reflecting differences in the local environments (Finkenstädt and Grenfell 1998; Grenfell and Bolker 1998; Langlois et al. 2001; Broadfoot et al. 2001).

Metapopulations provide a powerful framework for modeling disease dynamics for hosts that can be naturally partitioned into spatial sub-units.

The precise relationship between the force of infection for population i and the number of infectious individuals in population j depends on the assumed mechanism of transmission and the strength of interaction between the two populations. In general terms, the force of infection can be written as a sum:

$$\lambda_i = \beta_i \sum_j \rho_{ij} \frac{X_j}{N_i},$$

where the coefficients, ρ, are a measure of the strength of interaction between populations. Specifically, ρ_{ij} measures the relative strength of transmission *to* subpopulation i *from* subpopulation j. An important aspect of this formulation concerns the precise scaling with population size in the expression of λ_i. The equation above contains N_i in the denominator, which reflects the implicit assumption that transmission takes place in population i, presumably resulting from the movement of an infectious individual from population j. Alternatively, the assumption that transmission is due to a susceptible individual from population i picking up the infection during a temporary visit to population j would be incorporated by placing N_j in the denominator. The assumptions implicit in the coupling interaction are discussed more fully in Section 7.2.1.

The force of infection within a subpopulation can be expressed as a weighted sum of the prevalence in all populations.

We now explore the differences between deterministic and stochastic versions of this metapopulation model. Consider two large, fully susceptible populations ($S_1 = S_2 = 1$), with $\rho_{ii} = 1$ and ρ_{ij} much less than 1. (We will assume that the two populations are the same size, which simplifies the form of the coupling interaction, and ignore the effects of demography.) We start with an infectious disease solely in population 1, which exhibits a standard epidemic curve (Chapter 2), because the coupling between populations is assumed to be small. In the deterministic framework, ignoring births and deaths, the early dynamics of population 2 (before the proportion of susceptibles drops significantly, $S_2 \approx 1$) will be given by:

$$\frac{dI_2}{dt} = \beta_2 \rho_{21} I_1 + \beta_2 I_2 - \gamma_2 I_2.$$

This equation can be solved using the "integrating factor" (see, for example, Strang 1986) to obtain an expression for I_2 through time

$$I_2(t) = \int_0^t \beta_2 \rho_{21} I_1(s) \exp([\beta_2 - \gamma_2]s) ds. \tag{7.4}$$

This expression represents the exponential growth of prevalence in population 2 from time 0 to time t, due to the presence of $I_1(s)$ infecteds in population 1 at time s. The deterministic equation (7.4) has two main implications: the disease is "present" in population 2 from the start of the epidemic (in population 1), and the early infinitesimal infections that arrive in population 2 trigger an exponential growth at rate $\beta_2 - \gamma_2$.

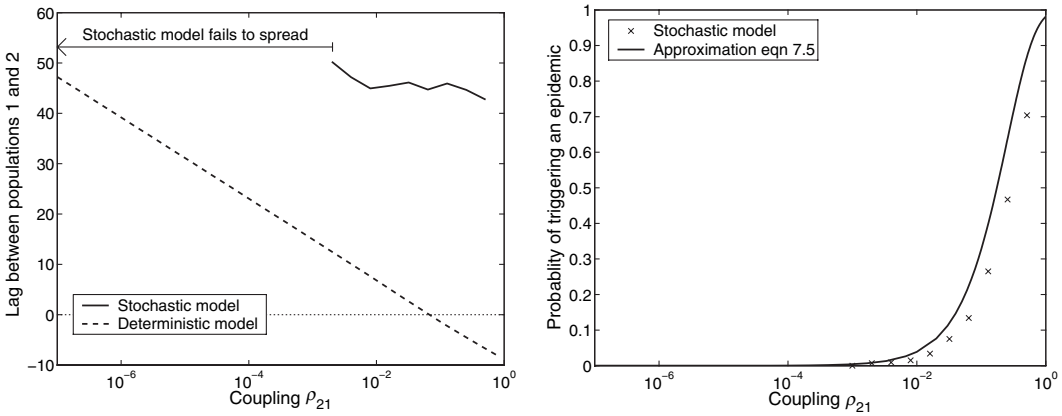

Figure 7.1. For a metapopulation with just two populations we examine the effect of coupling ρ_{21} on the dynamics of the epidemic in population 2. Population 1 is modeled deterministically and is initialized with $I(0) = 10^{-5}$, $S(0) = 1 - I(0)$. The left-hand graph shows the delay between the peak of the epidemic in population 1 and the peak in population 2, where population 2 is modeled either stochastically (solid line) or deterministically (dashed line) and is initially disease-free. The right-hand graph is the probability that a major epidemic is triggered in the stochastic population (crosses) compared to the analytical approximation, equation (7.5). ($\mu = \nu = 0$, $1/\gamma = 14$ days, $\beta = 0.3571$ per day $\Rightarrow R_0 = 5$, $\rho_{ii} = 1$, $\rho_{12} = 0$. Stochastic results are the average of 1,000 realizations, with population 1 treated deterministically, $N_2 = 10^5$).

In the analogous stochastic formulation, model behavior is significantly different. The probability that a major epidemic is triggered in population 2 is given by:

$$\begin{aligned}
\mathbb{P}(\text{epidemic}) &= \sum_{n=1}^{N} \mathbb{P}\,(\text{cases in 1 cause } n \text{ cases in subpopulation 2}) \times \\
&\qquad \mathbb{P}\,(n \text{ initial cases lead to a major epidemic}), \\
&= \sum_{n=1}^{N} \exp\left(-\beta_2\rho_{21}\int_0^\infty I_1(s)ds\right) \frac{\left(\beta_2\rho_{21}\int_0^\infty I_1(s)ds\right)^n}{n!} \times \left[1 - \left(\frac{\gamma}{\beta_2}\right)^n\right], \\
&= 1 - \exp\left(-\beta_2\rho_{21}\left[1 - \frac{\gamma}{\beta_2}\right]\int_0^\infty I_1(s)ds\right) \qquad (7.5) \\
&< 1 - \exp\left(-\beta_2\rho_{21}/\gamma\right).
\end{aligned}$$

So, in the stochastic formulation, if the coupling ρ_{21} between populations is small enough, there is a good chance that the epidemic will fail to spread (Park et al. 2002). When ρ_{21} is larger, although the pathogen may eventually spread, there may still be a significant delay before other populations are exposed. Hence, in stochastic metapopulation models, the spread of infectious disease is slower than for the deterministic counterpart.

This principle is illustrated in Figure 7.1. The pathogen is introduced in population 1 only, with $\rho_{ii} = 1$, and we measure the lag between the peak of the epidemic in population 1 and the subsequent peak in population 2. In both models, the delay between the peaks

decreases as the coupling ρ_{21} increases. For these parameters, however, it is not until the coupling exceeds approximately 0.01 that an epidemic has a significant chance of being triggered in the stochastic model. Two interesting aspects should be noted. The first is that for high levels of coupling, the lag in the deterministic model is negative (population 2 peaks first); this is because the force of infection in population 2 is boosted by the coupling from population 1, giving it a faster rate of epidemic growth (note that we have assumed that $\rho_{12} = 0$, so population 1 cannot receive infection from population 2). Second, the expected average lag predicted by stochastic simulations is far longer than the lag from the deterministic equations due to the chance nature of the initial transmission between populations.

With stochastic metapopulations, the spread of pathogen between subpopulations is reduced compared to the equivalent deterministic model.

7.2.1. Types of Interaction

We now turn our attention to the types of spatial transmission that are associated with different hosts and different types of movement. Although for convenience we label these as plant, animal, and human-commuter interactions, these descriptions are not rigid but rather illustrate the underlying host dynamics that generate the transmission terms. Hence, animal subpopulations that actually interact via occasional encounters would be better modeled as commuters, whereas animal subpopulations where the interaction is due to the wind-borne pathogen spread are more realistically modeled using the plant formulation.

In some circumstances, the interaction between subpopulations can be parameterized from direct observation, as is the case for commuter movements between communities (see Section 7.2.1.3) or from comparison to the recorded epidemic patterns (Wallace and Wallace 1993; Smith et al. 2002; Xia et al. 2004). Alternatively, the interaction terms between subpopulations are often assumed to obey a simple distance relationship (Erlander and Stewart 1990; Finkenstädt and Grenfell 1998).

7.2.1.1. Plants

The most obvious defining feature of plants (from an epidemiological perspective) that separates them from other hosts is that they do not move. This means that any spatial transmission must be wind- or vector-borne. We therefore retain the formulation

$$\lambda_i = \beta_i \sum_j \rho_{ij} I_j \tag{7.6}$$

and consider the coupling, ρ, as a function that decreases with the distance between the subpopulations, and for simplicity set $\rho_{ii} = 1$ (Park et al. 2001, 2002; Thrall et al. 2003). We can now calculate R_0 for infectious individuals in population i, as the expected number of secondary cases generated in all subpopulations:

$$R_0^i = \sum_j \frac{\beta_j \rho_{ji}}{\gamma_i}. \tag{7.7}$$

Note that the coupling term is now ρ_{ji} because we are concerned with transmission to j from i. It is important to realize that with this model, the addition of extra subpopulations

(with extra hosts) increases R_0. Intuitively, this is because more external populations can "capture" wind-borne pathogen particles that otherwise would not have contributed to the transmission process. However, dividing one subpopulation into two should not have the same effect—if population j is divided forming two new populations k and l, then $\rho_{ji} = \rho_{ki} + \rho_{li}$ so that R_0 remains constant. It is only the inclusion of additional host populations that can raise R_0.

The concept of a metapopulation is one that has been readily used by the plant research community, such that a variety of data exist on the distribution of diseases in plants (Burdon et al. 1995; Ericson et al. 1999) with a strong focus on the genetic specialization of the pathogen to local populations (Burdon and Thrall 1999; Bergelson et al. 2001).

Such coupling mechanisms are not exclusively for plant hosts, but can be applied to any sessile population with wind- or vector-borne pathogens. Hence, this form of metapopulation model is ideal for describing the spatial dynamics of livestock diseases, where each farm is a subpopulation and transmission between farms can either be wind-borne or due to the movement of people, vehicles, or animals (Keeling et al. 2001b; Ferguson et al. 2001a; Section 7.5.2).

For plants and other sessile hosts, coupling generally decreases with distance, mimicking the effects of wind- or vector-dispersal. Adding an extra subpopulation generally increases R_0 because more pathogens can be intercepted by the additional hosts.

7.2.1.2. Animals

For many animal populations, it is plausible to assume that the spread of disease is due to the migration or permanent movement of individuals. The simplest means of modeling this is to allow animals to randomly move between subpopulations (Foley et al. 1999; Broadfoot et al. 2001; Fulford et al. 2002), although other assumptions based on known dispersal behavior of specific species leading to different spatio-temporal dynamics may be more appropriate (Gudelj et al. 2004). The metapopulation SIR-type model is then:

$$\begin{aligned} \frac{dX_i}{dt} &= \nu_i - \beta_i X_i Y_i - \mu_i X_i + \textstyle\sum_j m_{ij} X_j - \sum_j m_{ji} X_i, \\ \frac{dY_i}{dt} &= \beta_i X_i Y_i - \gamma_i Y_i - \mu_i Y_i + \textstyle\sum_j m_{ij} Y_j - \sum_j m_{ji} Y_i. \end{aligned} \tag{7.8}$$

This is online program 7.1

Here, coupling is governed by the parameter m_{ij}, which measures the rate at which hosts migrate to subpopulation i from j—and therefore captures both emigration and immigration. We have assumed density-dependent transmission in equation (7.8), reflecting the common assumption about wildlife diseases—although frequency-dependent transmission could easily be accommodated. It is frequently assumed that the movement rates balance, $m_{ij} = m_{ji}$, so that the subpopulation sizes are maintained—there is no reason why this has to be the case and some subpopulations could act as sources of animals that colonize less favorable habitats. In this coupling framework (and assuming that β and γ are population independent and population sizes are equal or transmission is frequency dependent), the basic reproductive ratio is $\frac{\beta N}{\gamma+\mu}$ and is independent of the coupling strength. Intuitively, this is because each infectious animal transmits at a constant rate irrespective of which population it is in, and so always generates the same average number of secondary cases.

Compared to the plant models above, the movement of animals has two very different components: (1), it is the direct movement of infected animals that spreads the pathogen, and (2) the movement of susceptibles can help prevent stochastic extinctions (see Section 6.3.3) in heavily infected subpopulations. In this way, the coupling implied by animal movements is more variable than that due to wind or vector transmission assumed for plant infections. For the plant model (7.6), there is a continual force of infection from subpopulation 1 to subpopulation 2 (and vice versa); however, for the animal-based model (7.8) transmission between subpopulations occurs only following the movement of an animal. Therefore, in a stochastic framework either no infected animals have moved recently, in which case there is no transmission between populations, or an infected animal has moved, in which case the transmission is reasonably strong.

Models of animal diseases usually capture the transmission of infection by the permanent immigration and emigration of hosts. In these models R_0 is generally independent of the coupling because each host transmits infection at a constant rate.

7.2.1.3. Humans

For human populations, permanent relocation from one population to another is sufficiently rare that it may be ignored as an epidemiologically significant force. Instead, it is more natural to think about commuters spreading the disease (Keeling and Rohani 2002). Commuters live in one subpopulation but travel occasionally to another subpopulation. We therefore label X_{ij}, Y_{ij}, and N_{ij} as the number of susceptibles, infecteds, and total hosts currently in population i that live in population j. When there are multiple communities within the metapopulation, and when the populations are of different sizes or the strengths of interaction differ, it is more informative to return to first principles to calculate the dynamics. From the standard SIR models (Chapter 2) we consider the number of individuals of each type (S, I, and R) in each spatial class:

$$\begin{aligned}
\frac{dX_{ii}}{dt} &= \nu_{ii} - \beta_i X_{ii}\frac{\sum_j Y_{ij}}{\sum_j N_{ij}} - \sum_j l_{ji}X_{ii} + \sum_j r_{ji}X_{ji} - \mu_{ii}X_{ii},\\
\frac{dX_{ij}}{dt} &= \nu_{ij} - \beta_i X_{ij}\frac{\sum_j Y_{ij}}{\sum_j N_{ij}} + l_{ij}X_{jj} - r_{ij}X_{ij} - \mu_{ij}X_{ij},\\
\frac{dX_{ii}}{dt} &= \beta_i X_{ii}\frac{\sum_j Y_{ij}}{\sum_j N_{ij}} - \gamma Y_{ii} - \sum_j l_{ji}Y_{ii} + \sum_j r_{ji}Y_{ji} - \mu_{ii}Y_{ii},\\
\frac{dY_{ij}}{dt} &= \beta_i X_{ij}\frac{\sum_j Y_{ij}}{\sum_j N_{ij}} - \gamma Y_{ij} + l_{ij}Y_{jj} - r_{ij}Y_{ij} - \mu_{ij}Y_{ij},\\
\frac{dN_{ii}}{dt} &= \nu_{ii} - \sum_j l_{ji}N_{ii} + \sum_j r_{ji}N_{ji} - \mu_{ii}N_{ii},\\
\frac{dN_{ij}}{dt} &= \nu_{ij} + l_{ij}N_{jj} - r_{ij}N_{ij} - \mu_{ij}N_{ij},
\end{aligned} \tag{7.9}$$

This is online program 7.2

where l_{ij} measures the rate that individuals leave their home population j and commute to population i, and r_{ij} measures the rate of return. Frequently, in many human disease scenarios the parameters l and r can be found from commuter movement data or travel statistics (Grais et al. 2003; Cliff and Haggett 2004). Other parameters are allowed to

depend on both the home and current location—hence v_{ij} refers to individuals who live in location j but are born in location i. In these equations we have assumed frequency dependent transmission—as is the normal for human diseases—with $\sum_j N_{ij}$ giving the number of individuals currently in population i.

Using the formulation of equation (7.9), Figure 7.2 provides an example of an infectious disease spreading through the 67 counties of Great Britain. The simulations are initialized with the entire population of each county (as recorded in the 1991 census) being susceptible, and 10 infectious cases are placed in Inner London. The rates at which individuals commute l_{ij} are also taken from the 1991 census, while individuals are assumed to return home relatively quickly, at a rate of $r_{ij} = 2$ per day. Although this model is parameterized at a national level in terms of regular commuter movements, a similar modeling framework could be used to deal with the more irregular long-distance travel that can spread infection around the globe (Wilson 2003; Grais et al. 2003; Cliff and Haggett 2004).

Many factors emerge from Figure 7.2 that could be intuitively obvious without resorting to a spatial model: The first county to suffer a major epidemic is the source of initial infection, Inner London. Outer London peaks next due to its tight coupling to Inner London, and Outer London experiences the largest epidemic due to it having the largest population size. However, some elements may be more surprising: Greater Manchester and the West Midlands (along with West Yorkshire and Strathclyde) are among the last counties to have a sizable number of cases—despite their frequent interactions with London. This is attributable to the size of the population in these counties, such that although the infection may arrive relatively early it takes many weeks before the epidemic reaches its peak. Despite the clear delays between epidemics in different counties, within the first 50 days the infection has reached most areas (middle graph), after which time commuting plays a very minor role in the dynamics. This highlights the importance of rapidly imposing movement restrictions if we wish to curtail the spatial spread of infection. Additionally from this graph, it can be seen that the natural time to extinction is more than 300 days despite the fact that prevalence has dropped to very low levels within half this time. Finally, and as expected from simple models (such as shown in Figure 7.1), a deterministic version of this model predicts a faster speed of disease spread.

7.2.1.4. Commuter Approximations

Although equation (7.9) provides a full mechanistic description of the disease behavior, a large number of equations are frequently involved ($3n^2$ equations for n populations), and so it is informative to relate this model to the simpler ones defined earlier. In fact, Keeling and Rohani (2002) showed that for two populations of equal size and equal epidemiological characteristics, equation (7.9) can be simplified by assuming that all commuter movements are very rapid. In this case, the force of infection experienced by population i can be written as:

$$\lambda_i = \beta_i\big((1-\rho)I_i + \rho I_j\big) \qquad j \neq i. \tag{7.10}$$

The coupling parameter, ρ, can be defined in terms of the mechanistic movement of individuals by:

$$\rho = 2q(1-q), \tag{7.11}$$

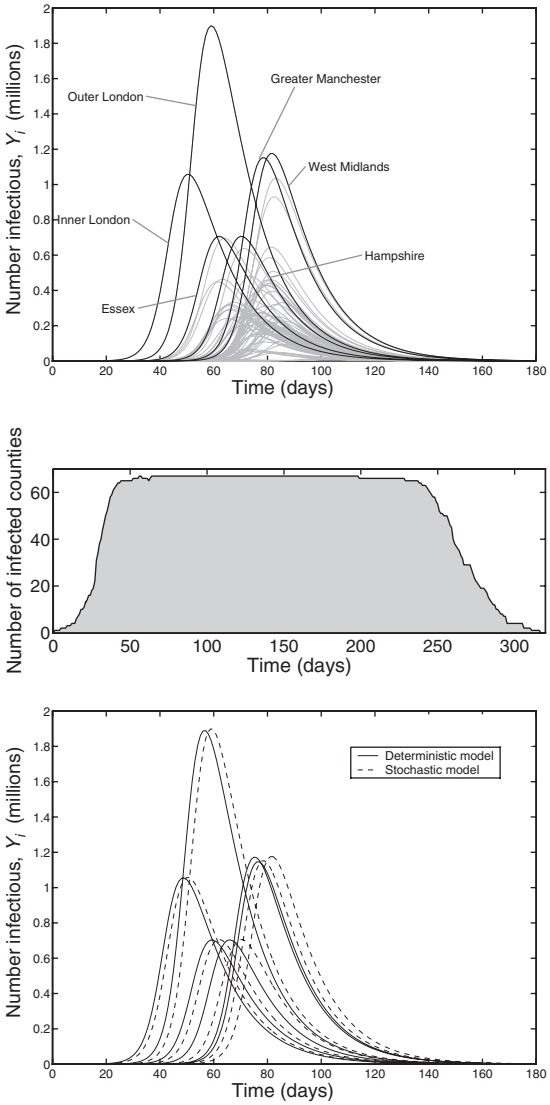

Figure 7.2. Deterministic and stochastic results for an infection spread through the 67 counties of Great Britain. The epidemic is initialized with 10 cases in Inner London, and is spread by commuter movements. The population size and rate of commuting is taken from the 1991 census database, and all trips are considered to be of short duration, $1/r = 0.5$ days. The top figure shows the county-level epidemics from a single stochastic iteration, with six counties highlighted. The middle graph shows the number of counties with infection from the same stochastic model. The bottom graph compares the deterministic solution (solid line) of equations (7.9) with the stochastic model (dashed line) for the six counties highlighted in the top graph. ($\mu = \nu = 0$, $1/\gamma = 14$ days, $\beta = 0.3571$ per day $\Rightarrow R_0 = 5$).

where q is the proportion of the time that individuals spend away in the other population,

$$q = l_{ij}/(r_{ji} + l_{ij}) = l_{ji}/(r_{ij} + l_{ji}).$$

Equation (7.11) is derived from the fact that when *either* the susceptibles of one population or infecteds of the other (but not *both*) move, there is a transfer of pathogen. We therefore find that ρ and hence the transfer of infection is maximized when individuals spend equal amounts of time in both home and away populations, $q = \frac{1}{2}$.

From this commuter approximation (equation (7.10)) it is clear that although increased coupling, ρ, leads to greater transmission between subpopulations, it weakens the transmission within subpopulations, therefore making R_0 independent of the coupling strength. Again, this type of disease transmission does not apply only to human commuters; Swinton et al. (1998) used a similar model to describe the spread of phocine distemper virus through harbour seals in the North Sea. In this context, haul-out beaches, where seals leave the water and congregate, act as natural subpopulations and infection was spread spatially by the occasional visits of seals to nearby beaches—thus the spread of infection is much closer to commuter-type movements than permanent migration usually associated with animals.

The spread of human diseases is best captured by the rapid commuter movements of individuals from their home subpopulation to another subpopulation and back again—requiring us to model both the current location and home location of individuals. When commuter movements are of short duration, this can be approximated by simple coupling. In these models, R_0 is independent of the coupling.

7.2.2. Coupling and Synchrony

Although coupling and the interaction between populations is key for the spatial invasion and spread of a disease, it also affects the endemic dynamics. In particular, the correlation between the disease dynamics in two subpopulations is generally a sigmoidal function of the interaction between them. Figure 7.3 shows the correlation against interaction strength for the four coupling mechanisms discussed above: equations (7.6), (7.8), (7.9), and (7.10). These results echo a general finding within metapopulation models, that the "interesting" spatial dynamics occur when the interaction is between 10^{-3} and 0.1 (Bolker and Grenfell 1995). When the interaction between subpopulations is too small the dynamics are effectively independent and spatial structure is unimportant, whereas when the interaction is too large the dynamics are synchronized, therefore, the subpopulations act like one large well-mixed population and again spatial structure is epidemiologically unimportant. The most notable factor in Figure 7.3 is the similarity between the results for different coupling mechanisms; once correctly scaled the correlation is a function of the interaction strength, with both the form of interaction and population size playing a relatively minor role. The scalings between interaction strengths are approximately:

$$\rho_{\text{plants}} \sim \frac{m}{\gamma + m} \sim 2\frac{l}{r + l}\left(1 - \frac{l}{r + l}\right) \sim \rho_{\text{commuters}}.$$

Hence, whereas commuter movements get scaled by their effective length of stay, permanent migration is multiplied by the average infectious period within the new subpopulation. In addition, although movement of susceptible commuters can lead to the

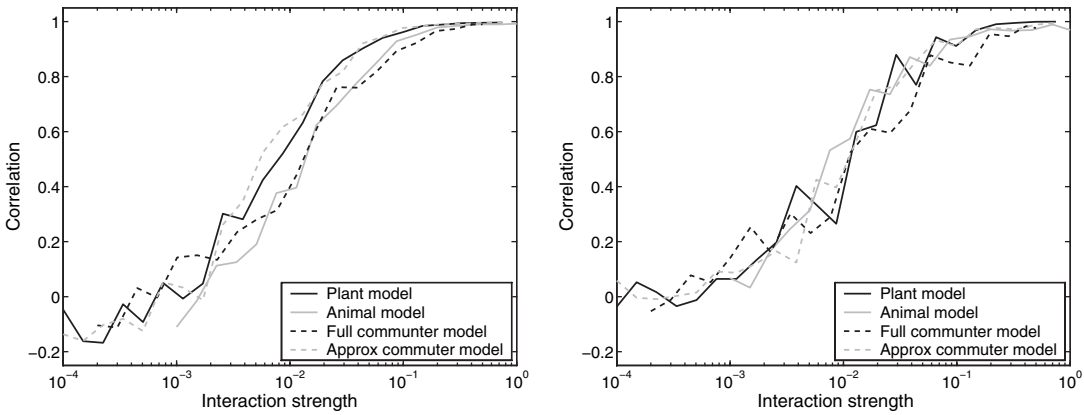

Figure 7.3. The correlation between the levels of an endemic disease in two stochastic populations for a range of interaction strengths and a variety of forms of interaction. It is clear that the correlation increases with the strength of interaction, and eventually asymptotes to one—when the population dynamics are synchronized. For the plant model (equation (7.6), solid black line) and the approximate commuter model (equation (7.10), dashed gray line), the x-axis is the coupling strength ρ. For the animal model (equation (7.8), solid gray line) the x-axis is $m/(\gamma + m)$ whereas, for the full commuter model (equation (7.9) dashed black line, $r_{ij} = r_{ji} = 1$), the x-axis is $2(p)(1-p)$, where $p = l/(l+r)$, which using equation (7.11) is equal to ρ for the approximate commuter model. ($\gamma = 0.1$, $\beta = 1$, stochastic imports at a rate $\varepsilon = 10^{-2}$, $\mu = 10^{-4}$, left-hand graph $v = 1 \Rightarrow N_i = 10^4$, right-hand graph $v = 10 \Rightarrow N_i = 10^5$).

transfer of infection between populations—because they can get infected while away and bring the disease home—leading to an additional factor of 2, the same is not true for the permanent migration of animals. Finally, although R_0 increases with coupling in the plant model (equation (7.7)) this effect is not strong enough to affect the correlation between populations.

The correlation between disease prevalence in two subpopulations increases sigmoidally with the strength of interaction between the populations. In general, the change from largely independent dynamics to synchrony occurs for interaction strengths from 10^{-3} to 0.1.

7.2.3. Extinction and Rescue Effects

Fundamental to the dynamics of any spatially segregated population is the pattern of localized extinction and subsequent colonization by rescue events (Foley et al. 1999; Boots and Sasaki 2002; Onstad and Kornkven 1992). As discussed in Chapter 6, smaller populations suffer a greater risk of extinction—intuitively, smaller populations will have fewer infected individuals and therefore be more prone to stochastic individual-level effects. In particular, the extinction risk has been seen to decrease exponentially with population size (Chapter 6; Bartlett 1957, 1960). This has clear implications for spatially segregated populations (and spatial models) where one large population has been subdivided into many smaller ones, with each small subpopulation facing a far greater risk of extinction. Therefore, in a metapopulation where there is no interaction or coupling, the disease in each of the small subpopulations will be rapidly driven extinct, leading to much

swifter global eradication than if coupling is large and the metapopulation was effectively randomly mixed. If we assume that the rate of extinction is proportional to $\exp(-\epsilon N)$, where N is the total population size, then the average time to extinction for the completely mixed (large coupling) metapopulation is:

$$\text{Time to extinction} = \frac{k}{e^{-\epsilon N}} = ke^{\epsilon N},$$

where k is the proportionality constant. In contrast, if the population is divided into n independent, noninteracting subpopulations (zero coupling), then the time to global extinction (in all subpopulations) becomes:

$$\text{Time to extinction} = \frac{k}{ne^{-\epsilon N/n}} + \frac{k}{(n-1)e^{-\epsilon N/n}} + \cdots + \frac{k}{e^{-\epsilon N/n}},$$

$$< k(1+\log(n))e^{\epsilon N/n},$$

which for persistent diseases ($e^{\epsilon N}$ much greater than 1) is far shorter as n becomes large. The above formula comes from calculating the average time to the first extinction when n subpopulations are infected, followed by the average time to the next extinction given that now only $n-1$ subpopulations are infected, proceeding iteratively until all populations are disease free.

Without interaction between the subpopulations, a spatially segregated metapopulation generally suffers a faster rate of stochastic extinction than its randomly mixed counterpart.

When the subpopulations interact, the behavior is far more complex. The transmission of infection to a disease-free subpopulation—termed a rescue event in the metapopulation literature (Hanski and Gilpin 1991, 1997; Hanski and Goggiotti 2004)—can allow the subpopulation to recover from extinction. In this way, long-term persistence can be achieved because infection is constantly reinvading subpopulations that have gone extinct. However, two antagonistic forces are in operation. Rescue events are clearly maximized when the rate that infection enters a subpopulation is large. Intuitively this requires that the interaction or coupling between the subpopulations is large. However, it also requires the populations to be asynchronous, such that when the disease is extinct in one population some of the others have ample infectious individuals; this occurs only when the interaction is fairly weak. As a result, tension exists between high levels of interaction but maintaining asynchrony, and therefore persistence can be maximized at an intermediate level of coupling. A comprehensive understanding of this problem has still not been reached. Keeling (2000b) and Hagenaars et al. (2004) have studied the level of stochastic extinction in two different models of disease metapopulations. The basic structure of the models is very similar, with only minor differences in the mechanism of spatial coupling; however, the two models are focused on diseases with very different properties and time scales. Keeling (2000b) focuses on acute infections comparable to measles, whereas Hagenaars et al. (2004) consider more persistent infections with longer infectious periods and lower R_0. In Figure 7.4, we show examples of the similarities and differences in model behavior reported in these two papers. Both models predict that, at the local scale, higher levels of coupling lead to the disease being present in the subpopulations for longer (less time disease-free, as shown in the top-left graph). However, at the global

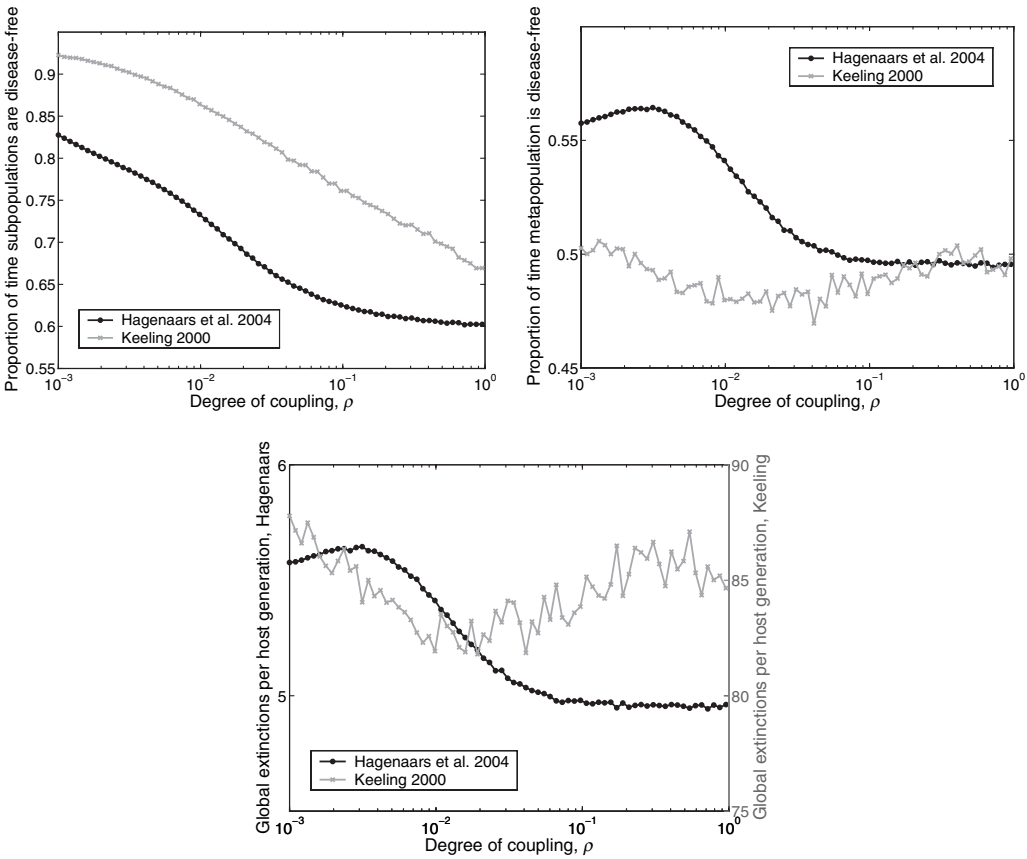

Figure 7.4. Comparison of how the extinction patterns change with the level of coupling from two models: Keeling (2000b) in gray and Hagenaars et al. (2004) in black. The top-left graph shows the proportion of the time that a subpopulation is disease free, whereas the top-right graph shows the proportion of the time that the entire metapopulation is disease free. The bottom graph shows the number of discrete global extinction events (the number of times the entire metapopulation becomes disease free) per host generation; note that the results from the two models are plotted at very different scales. The model of Hagenaars et al. (2004) deals with a small total population size ($N = 10{,}000$), with a relatively protracted infection ($1/\gamma = 125$ days, $R_0 = 5$) with infrequent imports ($\delta = 5 \times 10^{-5}$ day^{-1}; see Section 6.3.3.1), whereas the model of Keeling (2000b) the population size is slightly larger ($N = 30{,}000$), and the disease parameters are measles-like ($1/\gamma = 13$ days, $R_0 = 17$, $\delta = 9.3 \times 10^{-3}$ day^{-1}). In both models the birth and death rates are ($\nu = \mu N$, $\mu = 5 \times 10^{-5}$ day^{-1}), where the other parameters of the Hagenaars model have been scaled accordingly. In both models the population is split into 10 subpopulations.

scale, the two model predictions diverge. The model of Keeling (2000b) shows very little variation in the proportion of time the entire metapopulation is disease free and has a shallow minimum point at $\rho \approx 0.02$. In contrast, the model of Hagenaars et al. (2004) shows more variation and a clear minimum when the coupling is large, $\rho = 1$. Finally, when we focus on the number of global extinction events the Keeling model has again an interior minimum, whereas for the Hagenaars model extinctions are minimized at $\rho = 1$. In addition, extinctions are far more likely in the Keeling model. It is still a major

challenge to incorporate such results into a general framework, understanding how disease characteristics and spatial coupling interact to determine persistence.

When interaction between the subpopulations is included, the level of local (subpopulation scale) and global (metapopulation wide) extinctions is an emergent property of the dynamics and cannot be easily predicted from the disease parameters.

Rather than being an abstract concept, this problem has strong public health implications. The last century has seen far more national and international travel, increasing the coupling between populations (Grais et al. 2003; Cliff and Haggett 2004)—the implications of this for disease persistence and eradication needs to be studied using the form of metapopulation model developed here. Much more work is still needed to determine how population structure, disease dynamics, population size, infectious import rate, and coupling interact to determine disease persistence.

Two other applied problems are strongly related to the issues of coupling, synchrony and extinction. It has long been realized in conservation biology that increasing the mixing between populations, by introducing linking corridors of suitable habitat, is an effective means of conserving a species (Hanski 1999; Earn et al. 2000). However, these corridors may also act as a conduit for the spread of infection, and when facing a highly virulent pathogen, the presence of corridors may exacerbate the extinction of the host (Hess 1996). More recent, detailed work has called into question the strength of this result (Gog et al. 2002; McCallum and Dobson 2002), but the concept is still one that conservationists should consider.

A second applied problem concerns the dynamics of vaccinated metapopulations. Vaccination reduces the prevalence of infection within a population (Chapter 8), which increases its risk of extinction, and also reduces the effective interaction strength because less transmission of infection can occur. This reduction in the effective coupling in turn leads to less synchrony in the disease dynamics and therefore more effective rescue events (Earn et al. 1998; Rohani et al. 1999). This behavior is seen to some degree in the measles data set for England and Wales, where despite vaccinating at around 60% from 1970 to the mid-1980s the rates of stochastic extinction remained unchanged (Keeling 1997). Therefore, the effects of lower infection levels but greater asynchrony of epidemics effectively cancel. Pulsed vaccination (see Chapter 8) has been suggested as a mechanism of overcoming this problem where national vaccination campaigns for a few weeks each year will help to synchronize the dynamics and hence weaken the effect of rescue events (Agur et al. 1993; Nokes and Swinton 1997; Shulgin et al. 1998; Earn et al. 1998). Figure 7.5 shows the correlation (which measures the degree of synchrony) between two coupled populations under standard and pulse vaccination; clearly pulsed vaccination maintains the synchrony of epidemic behavior over of wide range of vaccination coverage.

Pulsed vaccination campaigns act to synchronize epidemics in coupled populations, and may lead to an increase in global extinction rates.

Extending these theoretical vaccination results into a practical public health tool is a challenge for the future. Pulsed vaccination clearly has the ability to synchronize epidemic behavior, which in turn limits the potential of rescue effects between coupled populations. It is hoped that such synchronization may increase the level of global extinctions at the metapopulation level and therefore promote the eradication of infection. Pulsed vaccination can also have significant logistical benefits when individual health care is limited, because

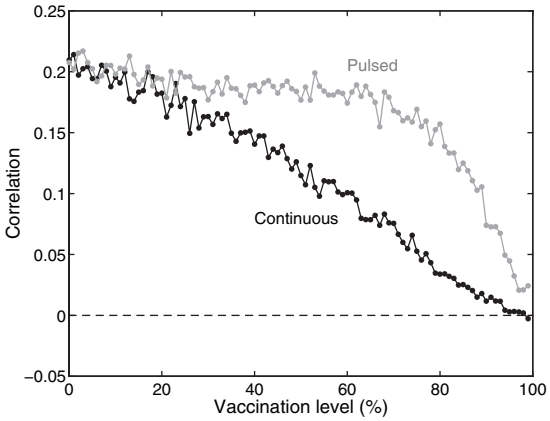

Figure 7.5. The correlation between two coupled populations with SIR-type infection as the level of vaccination is varied. For continuous vaccination (black), individuals are vaccinated at birth, whereas for the pulsed vaccination (gray) a comparable number of individuals are vaccinated every four years. Vaccination is assumed to offer lifelong protection. ($N = 100,000$, $\rho = 0.01$ with approximate commuter coupling, $1/\gamma = 10$ days^{-1}, $R_0 = 10$, stochastic imports $\delta = 5$ per year; see Section 6.3.3.1).

dedicated vaccination teams can be deployed. However, in the delay between the pulses there is the potential for many individuals to become infected. Clearly there is a trade-off: Frequent pulses (or continuous vaccination) limit the buildup of susceptibles, whereas infrequent, and therefore large, pulses have a greater synchronizing action. Determining the appropriate timing of vaccination pulses (or even a mixture of continuous and pulsed vaccination) requires the use of well-parameterized stochastic spatial models that also include age-structure—although the construction of such models can be pieced together from this chapter as well as Chapters 6 and 3, the parameterization and analysis of the possible control permutations is beyond the scope of this book.

7.2.4. Levins-Type Metapopulations

In the metapopulation models considered so far, the population levels within each subpopulation have been modeled explicitly—this may be computationally intensive. An alternative formulation was proposed by Levins (1969) where each subpopulation is simply defined as being either empty (disease-free) or occupied (having infection). There are clear parallels between this new classification of subpopulations, which ignores the precise prevalence and the traditional SIR classification of hosts, which ignores the level of pathogen. The intuitive way to conceptualize Levins-type metapopulations is to assume that localized extinctions and successful recolonization events are extremely rare, so that each subpopulation spends the vast majority of its time either disease free or close to the endemic equilibrium.

If we have a large number of subpopulations, and the coupling is global (so that each subpopulation has an equal probability of reinfecting any other subpopulations), then the probability that a subpopulation is infected, P, is given by:

$$\frac{dP}{dt} = \rho(1 - P)P - eP, \tag{7.12}$$

where ρ measures the reinfection (coupling) rate from an infected subpopulation to an uninfected one, and e is the rate of local extinction. Equation (7.12) is structurally identical to the SIS equation (Chapter 2), reflecting the fact that after a localized extinction the subpopulation is once again susceptible to infection.

When the subpopulations are of different sizes and the interactions are unequal, the above formulation can be refined such that P_i now refers to the probability that subpopulation i is infected.

$$\frac{dP_i}{dt} = \sum_j \rho_{ij}(1 - P_i)P_j - e_i P_i, \tag{7.13}$$

where different couplings can occur between different populations and the extinction rate (e_i) can also vary, often reflecting the population size. These rates can easily be used to translate this differential equation model into a stochastic one, with P_i being either zero or one.

Levins metapopulation models ignore the internal dynamics within each subpopulation, and instead classify each subpopulation as either infected or disease free.

Although the Levins formulation is intuitively appealing, the accuracy of the results is highly dependent on the assumption that extinction and successful recolonization events are rare compared to the standard epidemiological dynamics (Keeling 2000b). When this assumption breaks down, two confounding factors associated with the internal subpopulation dynamics become important. First, the conditions that lead to an extinction are unlikely to allow an immediate successful reinfection of the subpopulation. Second, following the extinction of infection the level of susceptibles increases; when there is a high proportion of susceptible individuals any subsequent infected is likely to be large and short-lived, rapidly returning to the disease-free state. Therefore, the timing between extinction and recolonization is vital (see Chapter 6, Figure 6.8). However, these discrepancies between the Levins approximation and the full stochastic metapopulation behavior are often during the early colonization dynamics, making the Levins models an ideal tool to study the spatio-temporal invasion of infection.

Despite differences between the equilibrium-level results of Levins and full metapopulation models, the Levins model still remains a useful and simple tool for studying invasion dynamics.

7.2.5. Application to the Spread of Wildlife Infections

We contrast the Levins metapopulation model with the full metapopulation model by considering two examples of invading wildlife diseases that have been tackled by the two differing approaches. The full metapopulation model of Swinton et al. (1998) was used to investigate the spread of phocine distemper virus around the North Sea coastline. Similar formulations have been used to describe the spread of bovine tuberculosis in badgers (White and Harris 1995), parapoxvirus in squirrels using a grid of stochastic subpopulations (Rushton et al. 2000), and rabies in foxes again using a grid of stochastic subpopulations (Tischendorf et al. 1998). The Levins metapopulation model of Smith et al. (2002) was used to explain the spread of rabies in the raccoon population of Connecticut.

7.2.5.1. *Phocine Distemper Virus*

In 1988, an epidemic of phocine distemper devastated the harbour seal (*Phoca vitulina*) populations in the North Sea (Dietz et al. 1989). Starting in Anholt, Denmark, in early April, the disease spread in a wave-like manner around the North Sea coastline, triggering epidemics from Norway to Ireland. The UK populations were the last to lose the disease in August of 1989, although the bulk of the cases occurred before the end of 1988.

Swinton et al. (1998) modeled this epidemic as a set of 25 subpopulations, mimicking the 25 locations (seal colonies) where infection was recorded. The dynamics of phocine distemper in this metapopulation were modeled as:

$$\begin{aligned}
\frac{dX_i}{dt} &= -\beta X_i \left[(1-\rho)\frac{Y_i}{N_i} + \rho \frac{\sum_{j=i-1,\,i,\,i+1} Y_j}{\sum_{j=i-1,\,i,\,i+1} N_j} \right] - \mu X_i, \\
\frac{dW_i}{dt} &= \beta X_i \left[(1-\rho)\frac{Y_i}{N_i} + \rho \frac{\sum_{j=i-1,\,i,\,i+1} Y_j}{\sum_{j=i-1,\,i,\,i+1} N_j} \right] - \sigma W_i - \mu W_i, \\
\frac{dY_i}{dt} &= \rho W_i - \gamma Y_i - m Y_i - \mu Y_i, \\
\frac{dZ_i}{dt} &= \gamma Y_i - \mu Z_i,
\end{aligned} \tag{7.14}$$

where $\frac{m}{m+\gamma} \approx 0.2$ gives the probability of mortality from the infection. Swinton et al. simulated this model stochastically and were able to estimate the majority of the parameters needed from good observational data; however, the coupling parameter, ρ, could be found only by matching the model to the observed wavespeed, leading to $\rho \approx 0.1$. The precise form of coupling used in these equations differs from the standard assumptions and therefore requires some explanation. The first term reflects that a fraction $(1-\rho)$ of infectious seals remain at their haul-out site and can therefore infect susceptible seals—the transmission is assumed to be frequency dependent, due to the types of interaction that occur at haul-out sites. The second transmission term is due to encounters with seals at sea, away from the main haul-out sites; again, frequency-dependent transmission is assumed. Therefore, although the formulation of the transmission terms is unusual it reflects the form of interaction between seals. Figure 7.6 shows the wavelike progress of the invading infection; because this is a stochastic model, no two simulations will be identical but the general wave-speed is largely invariant.

Two difficulties exist with this model formulation. First, all subpopulations (seal colonies) are given identical parameters and population sizes. Therefore, heterogeneities that may account for epidemiologically important factors, such as the prolonged epidemic observed in Tayside, are ignored. Second, the model is essentially one-dimensional with nearest-neighbor coupling (see Section 7.3.1); therefore, the true spatial structure has been neglected and the different distances between seal colonies ignored. However, despite these limitations, the model provides a simple means of assessing the spatio-temporal dynamics of phocine distemper epidemics.

7.2.5.2. *Rabies in Raccoons*

The spread of rabies has been extensively studied using spatial models building upon the pioneering work of Murray et al. (1986), which formulated PDE models (see Section 7.4)

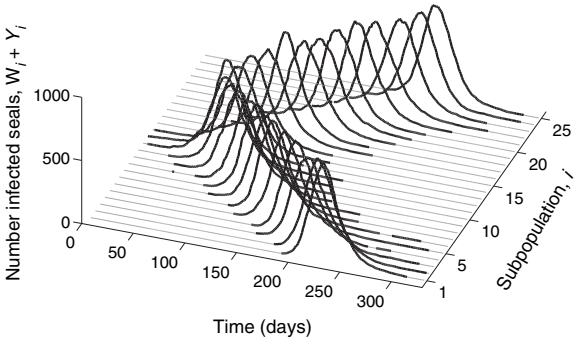

Figure 7.6. Results of a stochastic simulation of the phocine distemper metapopulation model, equation (7.14), as proposed by Swinton et al. 1998. The number of infected seals in each subpopulation is shown, with black lines used when at least one seal is infected. In this model births and deaths have been ignored for simplicity. ($\beta = 0.4$, $\rho = 0.1$, $\sigma = 0.1428$, $\gamma = 0.1143$, $m = 0.0286$, $\mu = 0$, $N_i(0) = 2000$).

to understand the spread of rabies in the fox population of Europe. At a smaller scale, Smith et al. (2002) used a Levins-type metapopulation model to study the spread through Connecticut of rabies in racoons from 1991–1996, concentrating on the underlying spatial heterogeneity of the habitat. This spread is part of a larger wave of infection that began along the Virginia/West Virginia border in the mid-1970s.

Using a similar format as equation (7.13), Smith et al. model the state of the 169 townships in Connecticut, and for township i define the stochastic rate of infection as

$$\varepsilon_i(1 - P_i) + \sum_j \rho_{ij}(1 - P_i)P_j, \tag{7.15}$$

where P_i is one if the racoons in the township are infected and zero otherwise. Unlike the previous Levins metapopulation model (7.13), the localized extinction of infection has been ignored. Here ε_i measures the random long-distance dispersal of rabies due to racoon translocation and ρ_{ij} measures local transmission between adjacent townships (see Figure 7.7). Here $\rho_{ij} = A$ if townships i and j share a land-boundary, $\rho_{ij} = B$ if the townships are separated by a river, otherwise $\rho_{ij} = 0$. This stochastic model (which is an SI model because there is no recovery or local extinction of infection) was compared to the observed first recorded case of rabies in each township, in order to determine suitable coupling and long-range transmission parameters. The simplest model that provides a reasonable fit to the observed data had $\varepsilon_i = 2 \times 10^{-4}$, $A = 0.66$, and $B = 0.09$ (all rates in months), showing that rivers reduce transmission by 87% compared to land boundaries and that local transmission accounts for the vast majority of spatial spread. Other, more complex model formulations included the size of the human population as a proxy for the density of racoons within a township; such models suggest that population density plays a small but positive role in transmission.

Figure 7.8 shows the impact of these three different coupling parameters. Rivers clearly have a significant impact on the spatial spread of infection, especially when long-range translocations are impossible (gray line and middle map). When the impact of rivers is ignored (dashed line and right map), the speed of spatial spread is far more rapid, infecting the entire state in two-thirds of the time. Interesting, although the value of ε is very small, its effect is significant because it breaks the assumption of strict local transmission.

Figure 7.7. The 169 townships within Connecticut showing the initial site of the first recorded cases in Ridgefield Township, the forcing on the western townships due to infection from neighbouring New York, and the position of rivers (black) which act as a natural barrier to the movement of rabid racoons.

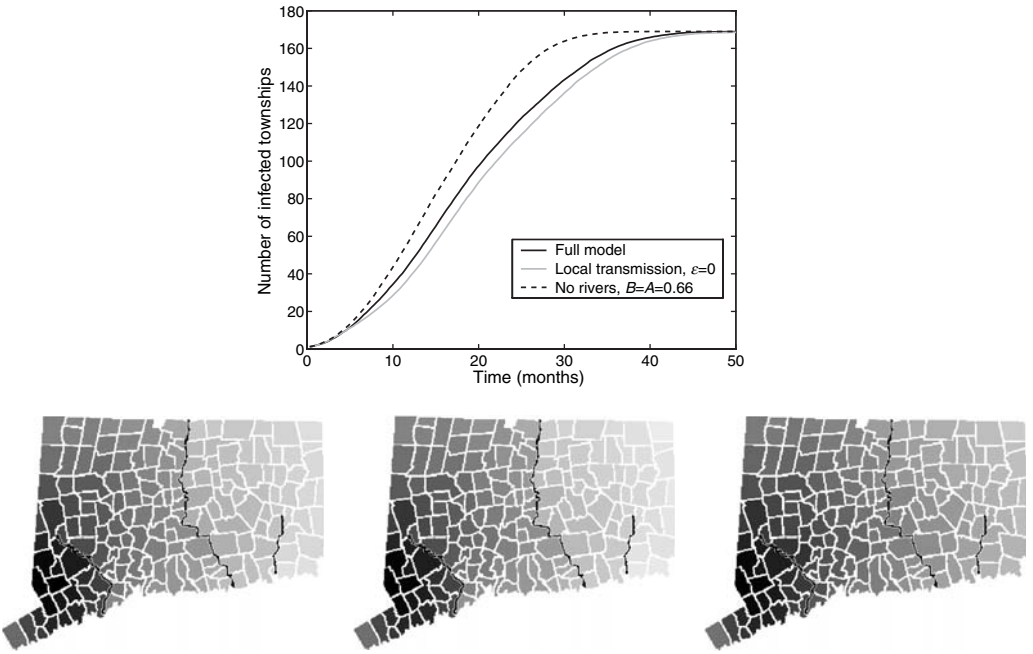

Figure 7.8. The effect of the various coupling terms on the spatial spread of rabies in Connecticut, based on the model and parameterization of Smith et al. (2002). To simplify the dynamics, forcing from New York state is set to zero. The top graph shows the average number of infected townships as a function of time from the initial seeding of infection. Three different assumptions about coupling are shown: the full model ($A = 0.66,\ B = 0.09,\ \varepsilon = 2 \times 10^{-4}$), a model with local transmission only ($A = 0.66,\ B = 0.09,\ \varepsilon = 0$), and a model where rivers had no impact on transmission ($A = 0.66,\ B = 0.66,\ \varepsilon = 2 \times 10^{-4}$). The spatial pattern for these three models is illustrated on the three maps, with darker colors representing earlier average infection times.